*Canadian Mineralogist*
Vol. 16, pp. 207-221 (1978)

# FLUORIDE–HYDROXYL RATIOS OF SKARN SILICATES, CANTUNG E–ZONE SCHEELITE OREBODY, TUNGSTEN, NORTHWEST TERRITORIES

U KHIN ZAW[1] AND ALAN H. CLARK
*Department of Geological Sciences, Queen's University, Kingston, Ontario K7L 3N6*

## ABSTRACT

In the major Cantung E–Zone exoskarn orebody, scheelite was deposited in equilibrium with, successively, clinopyroxene+garnet, actinolite and biotite, at mean temperatures (from fluid inclusion homogenization) of 487°, 433° and 415°C, respectively, and under a confining pressure of 1000 bars (from sphalerite geobarometry). The fluorine contents of skarn biotites and actinolites are in the ranges 0.82–2.99 and 0.25–0.90 wt.%; Mg/Mg+Fe and F/OH+F ratios are positively correlated in both minerals. Application of the experimental data of Ludington & Munoz (1975) for fluoride:hydroxyl exchange between biotite and fluid yields a value for log $f(H_2O)/f(HF)^{fluid}$ of 4.5±0.3; thus, $f$(HF) was approximately 0.009 bars during the final stage of mineralization. The compositions of Fe– and Al–rich magmatic biotites from a nearby pluton are inferred to have equilibrated at *ca.* 550°C with fluids which generated clinopyroxene+garnet skarns; this suggests that $f$(HF) was maintained at this low level throughout the evolution of the E–Zone orebody. The comparative F:OH exchange in actinolitic amphiboles is in broad agreement with published estimates, but is not tightly constrained by the Cantung assemblages. Although not ruling out the possibility of tungsten solution in the form of an aqueous fluoride complex, the low HF fugacity inferred for the E–Zone hydrothermal fluids lends no support to this mode of transport.

## SOMMAIRE

Dans le gîte de type exoskarn de la zone E de Cantung, Territoires du Nord-Ouest, la schéelite s'est formée successivement en équilibre avec clinopyroxène + grenat, actinote et biotite, à des températures moyennes de 487°, 433° et 415°C (homogénéisation d'inclusions fluides) sous une pression de 1000 bars (géobarométrie de la sphalérite). Les biotites et les actinotes des skarns contiennent respectivement de 0.82 à 2.99 et de 0.25 à 0.90% (en poids) de fluor. Les rapports Mg/(Mg+Fe) et F/(F+OH) sont en corrélation positive dans chaque minéral. L'application des données expérimentales de Ludington & Munoz (1975) sur l'échange fluorure:hydroxyle entre biotite et fluide donnent une valeur de 4.5±0.3 au rapport log $f(H_2O)/f(HF)$, pour le fluide; on avait donc $f(HF) = 0.009$ bars au stade final de la minéralisation. Les compositions de biotites magmatiques riches en Fe et en Al d'un massif plutonique voisin auraient été en équilibre, à environ 550°C, avec les fluides qui ont donné naissance aux skarns à clinopyroxène + grenat, ce qui indiquerait une faible valeur de $f$(HF) pendant toute l'évolution du gîte. Les résultats comparatifs obtenus sur l'échange F:OH dans les actinotes concordent généralement avec les estimations publiées. La faible valeur de la fugacité HF attribuée aux fluides hydrothermaux de la zone E n'exclut pas la possibilité d'une mise en solution du tungstène sous forme de complexe de fluorures aqueux, mais n'étaye en rien l'hypothèse de pareil mode de transport.

(Traduit par la Rédaction)

## INTRODUCTION

Although there has been considerable interest in the role of fluorine in the formation of contact-metasomatic mineralization in general, and in the hydrothermal transport of tungsten in particular (*e.g.*, Bryzgalin, 1958; Ivanova 1966; Burt 1972; Foster 1977), few have investigated the abundance and distribution of this halogen in hydroxyl-bearing silicate minerals in scheelite skarn ore deposits. In one of the few relevant studies, Darling (1971) determined the fluorine content of magmatic biotites in stocks associated with the large Pine Creek, California, scheelite deposits, but did not investigate the compositions of skarn silicates. In the field of applied geochemistry, Cachau-Herreillat & Prouhet (1971) delimited fluorine anomalies in soils in the vicinity of scheelite-bearing skarns at Salau, in the French Pyrénées, but there is limited agreement regarding the general efficacy of such an approach.

Whereas Troll & Gilbert (1972) encountered difficulties in their experimental study of fluoride-hydroxyl exchange between aqueous fluids and members of the tremolite–ferroactinolite series, Munoz & Ludington (1974) demonstrated

[1]Present address: Department of Applied Geology, Rangoon Natural Science University, Rangoon, Burma.

the dependence of the F:OH ratio of biotite on the $f(H_2O)/f(HF)$ ratio of the fluid, on temperature, and on the cationic composition of the mica. Subsequently, Ludington & Munoz (1975) presented revised data on biotite:fluid F-OH exchange, whereas Munoz & Ludington (1977) have recently carried out comparable experiments with muscovite. As a result, mica compositions may be employed to estimate the $f(H_2O)/f(HF)$ ratio of an ore-forming aqueous fluid, although some uncertainties persist in the interpretation of the experimental data.

In this paper, we provide analytical data for F:OH ratios of hydrothermal biotites and calciferous amphiboles from the Cantung E–Zone scheelite skarn orebody, located at Tungsten, Northwest Territories (Lat. 61°57′N.; Long. 128°15′ W.). This is one of the world's major sources of tungsten concentrates, with ore reserves of over 4 million tons at 1.55% $WO_3$ (*Mining J.* of May 13, 1977); the deposit has been the subject of a detailed petrological study (Zaw 1976; Zaw & Clark 1977). The temperatures and confining pressures of formation of biotite and amphibole associated with scheelite have here been delimited by fluid-inclusion homogenization and application of the sphalerite geobarometer (Scott 1973). This approach provides an opportunity to estimate, from the fluoride contents of the biotites, the $f(H_2O)/f(HF)$ ratio of a natural, ore-forming aqueous fluid under unusually well-controlled conditions, and to delimit the comparative F:OH exchange in members of the calciferous amphibole series.

A detailed description of the Cantung E-Zone orebody and its setting is in preparation; the geological background will herein be presented only in sufficient detail for clarification of the fluorine distributions.

## Geological Relationships

The Logan–Mackenzie Mountain belt along the Yukon-Northwest Territories border forms a major part of the Mackenzie fold belt, a segment of the Foreland fold and thrust belt of the northern Columbian orogen (Wheeler & Gabrielse 1972). Predominantly shallow-water Proterozoic and Paleozoic sediments, originally deposited across the transition between the southwesterly trending Selwyn basin and the northeasterly Mackenzie or Redstone arch, were most intensely deformed in the course of the Mesozoic Columbian orogeny. Post-tectonic granitoid batholiths and plutons were emplaced in late Cretaceous time (Gabrielse & Reesor 1974). Economic scheelite mineralization in this arc occurs characteristically as clinopyroxene-garnet exoskarn bodies and generally, but not entirely, within Cambrian carbonate horizons and related spatially to these intrusions. The largest tungsten reserves are contained in the Mactung deposit, but the Cantung mine, operated by Canada Tungsten Mining Corporation, has been the sole producer.

At Cantung, folded and very weakly metamorphosed pelites and limestones of Lower Cambrian age (Blusson 1968) overlie Hadrynian(?) phyllites (the "Lower Argillite"), and have been intruded by large stocks made up predominantly of quartz monzonite (Blusson 1968, Zaw 1976). Economic exoskarn mineralization, comprising skarn silicates and hexagonal pyrrhotite with lesser scheelite and minor chal-

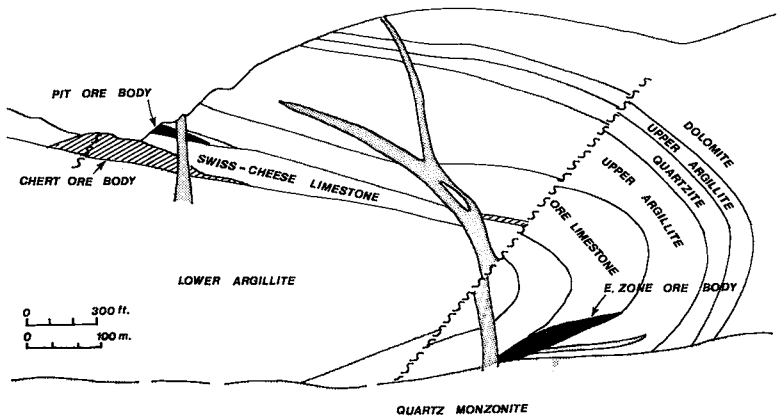


FIG. 1. Simplified north-south geological cross-section through the E–Zone and Pit orebodies, Cantung, N.W.T. (after Canada Tungsten Mining Corp. Geological Department). North is to the right.

copyrite, occurs as massive lenses, veins and stockworks at two locations in the so-called Ore Limestone, a relatively pure carbonate unit of the Lower Cambrian succession (Fig. 1). Of the two mineralized zones, the Open–Pit orebody, now mined out, consisted almost wholly of clinopyroxene–garnet skarn (Blusson 1968), and was formed adjacent to a microgranitic dyke some 330 metres above the broadly flat-lying roof of the Mine Stock.

Skarn of this type also occurs underground in the newly-developed E–Zone orebody, which lies immediately above the intrusive contact (Fig. 1). Here, however, the pyroxene–garnet association constitutes only a hanging-wall zone to the orebody, underlain by a central zone rich in amphibole, and by a footwall skarn in which coarse-grained biotite predominates. The boundaries between these three main skarn zones are irregular, but crudely parallel to the roof of the underlying stock, which is cross-cut by numerous scheelite-bearing, though uneconomic, quartz veins with greisened selvedges.

Megascopic and microscopic textural relationships demonstrate that the sequence of skarn formation within the E-Zone was: 1) clinopyroxene–garnet skarn; 2) amphibole skarn, and 3) biotite skarn, which overlapped with the development of the quartz-vein systems. Although the two "hydrous" skarn assemblages bear, in part, a replacive and retrograde relationship to the early clinopyroxene–garnet skarn, we consider that a large proportion of the later skarn and ore was emplaced through direct replacement of contact-metamorphosed marbles. Certainly, scheelite and sulfides were introduced anew at each skarn stage, and display no textural evidence of instability in any of the three zones.

The successive stages of skarn emplacement have been shown by fluid-inclusion data to have taken place at progressively lower temperatures. Homogenization runs on primary liquid–gas inclusions of low salinity in quartz, scheelite and clinopyroxene yield temperatures in the range of 520–455°C (mean 487°C) for the pyroxene–garnet skarn, of 464–371°C (mean 415°C) for the biotite skarn, and of 452–350°C (mean 405°C) for the quartz veins. The observed temperature ranges are represented on the scale of individual hand specimens, and are regarded tentatively as indicating actual crystallization-temperature intervals for the different stages. Few successful homogenization runs have been carried out for the amphibole skarn, but a range of 440–421°C (mean 433°C) was obtained for several inclusions in a single specimen.

The filling temperatures of fluid inclusions presented above have been corrected for a confining pressure of 1000 bars on the basis of the FeS content of sphalerite occurring in contact with hexagonal pyrrhotite and pyrite in a quartz vein associated with the biotite skarn.

K-Ar dating (Archibald *et al.* 1978) has yielded apparent ages of 89.2±9.4 to 92.3±2.5 Ma for micas from the quartz monzonite pluton and from later stages of mineralization. It is proposed, therefore, that intrusion and hydrothermal mineralization took place at shallow depths over a relatively brief time span in the Upper Cretaceous, and that the locus of skarnification and mineralization migrated *towards* the roof of the Mine Stock as it cooled.

## Micas and Amphiboles of the E-Zone Skarns

### *Petrographic relationships*

The micas and calciferous amphiboles associated with scheelite–sulfide mineralization in the E-Zone orebody display wide variations in color in hand-specimen. The micas range from medium green to yellowish to dark brown, and the amphiboles consist of very pale green and dark green to blackish varieties. In hand specimen, the micas seem chloritized or oxidized, but they look essentially fresh in thin section, although minor chlorite and sericite are observed in some samples. The amphiboles locally exhibit partial replacement by fine-grained biotite, but are generally unaltered. The skarn minerals range in habit from fine-grained aggregates to very coarse flakes or fibrous-columnar prisms intimately intergrown with calcite, quartz, pyrrhotite and the economic minerals scheelite and chalcopyrite. Fluorapatite, idocrase and tourmaline are persistent, generally minor constituents of the skarns. Magnetite has not been observed as a component of these assemblages, and pyrite is rare, being most abundant in a few late-stage veins. Fluorite has been recorded as a minor phase in one diamond-drill hole from above the E-Zone, but is apparently absent in the orebody itself.

Biotite characteristically occurs in, and along the selvedges of late-stage quartz veins cutting the E-Zone skarns, whereas amphiboles are less common in such settings. The quartz veins contain, in addition to minor scheelite and sulfides, microcline, amphibole, chlorite, calcite, tourmaline and plagioclase.

In both amphibole and mica skarns, scheelite occurs predominantly as relatively coarse-grained pyramidal subhedra and euhedra, intergrown with the main silicate minerals, or interstitial to

them. The textural relationships suggest that the scheelite and silicates were deposited simultaneously, whereas the sulfides tend to display a more consistently interstitial distribution with respect to the silicates.

The hand-specimen heterogeneity of both major skarn silicates is paralleled by their microscopic appearance. Thus, the amphibole ranges from almost colorless or pale green and very weakly pleochroic, to dark green, and strongly pleochroic in thin section. The $2V$ of all amphiboles lies between 75° and 80°. The paler members have $z \wedge c$ 5°–10°, whereas he darker have $z \wedge c$ up to 20°. It is noteworthy that scheelite exhibits a preferential association with the darker amphiboles, and zones in which the pale amphibole predominates are commonly essentially barren.

The brown skarn micas exhibit strong pleochroism from orange brown ($Z$ and $Y$) to pale yellow or nearly colorless ($X$), whereas the green variety ranges from plate green ($X$) and yellowish green ($Y$) to light brownish green ($Z$). Both forms are optically negative, and their $2V$ varies from 0° to 15°. Neither scheelite nor sulfides show a preferential association with either mica type.

*Analytical methods*

Partial analyses were carried out on nine skarn amphiboles and ten micas, using an Applied Research Laboratories AMX electron microprobe. Major elements, with the exception of fluorine, were determined by energy-dispersive analysis, using standards whose energy spectra had been previously stored on magnetic tape, and employing an accelerating potential of 15 kV, a beam current of $0.34 \times 10^{-7}$A, a beam diameter of 5-7$\mu$m, and a counting interval of 120 secs. At least six separate analyses were averaged to yield each analysis given in Tables 1, 2. Mineral grains were checked for homogeneity prior to analysis. Raw data for Si, Ti, Al, Fe, Mg, Mn, Ca, Na and K were initially corrected on an NS-880 minicomputer using a multiple least-squares routine. The intensity ratios were corrected for matrix effects following Bence & Albee (1968), as well as for drift, using a Fortran correction program developed by P. L. Roeder (priv. comm.). This program was modified by J. M. Allen (priv. comm.) to accommodate the matrix effect of $H_2O$ in hydrous silicates. Alpha factors used in the iterative correction procedure were taken from Albee & Ray (1970). The accu-

TABLE 1. ELECTRON MICROPROBE PARTIAL ANALYSES AND STRUCTURAL FORMULAE OF SKARN AMPHIBOLES, E-ZONE OREBODY

| Weight % | (1) | (2) | (3) | (4) | (5) | (6) | (7) | (8) | (9) |
|---|---|---|---|---|---|---|---|---|---|
| $SiO_2$ | 57.57 | 53.32 | 51.63 | 55.62 | 53.53 | 55.87 | 57.47 | 56.07 | 51.53 |
| $Al_2O_3$ | 0.51 | 4.39 | 4.37 | 0.97 | 4.71 | 1.19 | 0.05 | 0.81 | 4.42 |
| $TiO_2$ | 0.00 | 0.09 | 0.31 | 0.01 | 0.07 | 0.04 | 0.08 | 0.08 | 0.22 |
| FeO* | 5.35 | 14.57 | 15.09 | 11.41 | 13.83 | 9.38 | 4.67 | 7.57 | 15.67 |
| MgO | 19.54 | 12.26 | 12.40 | 17.53 | 12.13 | 18.35 | 21.48 | 19.58 | 12.90 |
| MnO | 0.57 | 1.23 | 1.22 | 0.75 | 0.63 | 0.73 | 0.32 | 0.19 | 0.89 |
| CaO | 12.50 | 11.48 | 11.47 | 12.09 | 11.75 | 12.25 | 12.99 | 12.59 | 11.48 |
| $Na_2O$ | 0.34 | 0.54 | 0.73 | 0.14 | 0.51 | 0.03 | 0.04 | 0.39 | 0.55 |
| $K_2O$ | 0.11 | 0.39 | 0.42 | 0.12 | 0.35 | 0.17 | 0.07 | 0.20 | 0.32 |
| F | 0.90 | 0.44 | 0.39 | - | 0.25 | 0.45 | 0.78 | 0.69 | 0.42 |
| $H_2O$** | 1.71 | 1.87 | 1.86 | 2.12 | 1.95 | 1.91 | 1.79 | 1.80 | 1.85 |
| Total | 98.72 | 100.37 | 99.73 | 100.76 | 99.60 | 100.18 | 99.41 | 99.68 | 100.03 |
| numbers of ions on the basis of 24 (O, OH, F) | | | | | | | | | |
| Si | 8.078 | 7.708 | 7.571 | 7.875 | 7.745 | 7.884 | 7.994 | 7.894 | 7.533 |
| $Al^{iv}$ | -0.078 | 0.292 | 0.429 | 0.125 | 0.255 | 0.116 | 0.006 | 0.106 | 0.467 |
| $Al^{vi}$ | 0.162 | 0.456 | 0.326 | 0.037 | 0.548 | 0.082 | 0.003 | 0.029 | 0.295 |
| Ti | 0.000 | 0.009 | 0.034 | 0.001 | 0.007 | 0.004 | 0.008 | 0.008 | 0.024 |
| $Fe^{+2}$ | 0.627 | 1.762 | 1.850 | 1.351 | 1.673 | 1.107 | 0.543 | 0.891 | 1.916 |
| Mg | 4.087 | 2.642 | 2.711 | 3.700 | 2.617 | 2.860 | 4.454 | 4.109 | 2.811 |
| Mn | 0.068 | 0.151 | 0.152 | 0.090 | 0.077 | 0.087 | 0.038 | 0.023 | 0.110 |
| Ca | 1.879 | 1.778 | 1.802 | 1.834 | 1.821 | 1.852 | 1.936 | 1.899 | 1.798 |
| Na | 0.093 | 0.150 | 0.207 | 0.038 | 0.143 | 0.008 | 0.011 | 0.106 | 0.155 |
| K | 0.020 | 0.071 | 0.078 | 0.022 | 0.065 | 0.031 | 0.012 | 0.036 | 0.060 |
| F | 0.40 | 0.199 | 0.181 | - | 0.114 | 0.201 | 0.343 | 0.307 | 0.192 |
| OH | 1.60 | 1.798 | 1.819 | 2.00 | 1.886 | 1.799 | 1.657 | 1.693 | 1.808 |

* Total iron reported as FeO. ** $H_2O$ was calculated assuming F+OH ≡ 2

Sample numbers and localities

1) DDH-TRU 42-20A, at 98'; 2) DDH-ATU 64-20C, at 224'; 3) DDH-ATU 43-35E, at 129'; 4) 74-ACT-5, 1153-071 North Ramp; 5) DDH-ATU-24, at 145'; 6) 74-UG-24, Near Station 107, 1201-092 East Drift; 7) 74-UG-21, Near Station 96, 1201-092 East Drift; 8) 74-UG-10, Near Station 94, 1201-092 East Drift; 9) 74-ZKS-2, 1103-080 West Ramp.

TABLE 2. ELECTRON MICROPROBE ANALYSES AND STRUCTURAL FORMULAE OF SKARN MICAS, E-ZONE OREBODY

| Weight % | (brown) (1) | (brown) (2) | (brown) (3) | (brown) (4) | (brown) (5) | (green) (6) | (green) (7) | (green) (8) | (green) (9) | (green) (10) |
|---|---|---|---|---|---|---|---|---|---|---|
| $SiO_2$ | 40.56 | 39.78 | 41.39 | 40.97 | 39.10 | 40.79 | 40.02 | 41.51 | 41.36 | 41.79 |
| $Al_2O_3$ | 14.90 | 16.30 | 14.63 | 12.49 | 16.67 | 13.65 | 12.74 | 14.42 | 12.53 | 13.64 |
| $TiO_2$ | 0.00 | 0.00 | 0.02 | 0.00 | 0.80 | 0.06 | 0.00 | 0.00 | 0.00 | 0.06 |
| FeO* | 16.61 | 16.59 | 14.11 | 13.66 | 16.65 | 15.27 | 14.51 | 14.62 | 11.86 | 15.27 |
| MgO | 14.14 | 13.34 | 15.46 | 18.44 | 12.79 | 15.53 | 18.72 | 15.18 | 19.30 | 15.53 |
| MnO | 0.64 | 0.66 | 0.72 | 0.21 | 0.56 | 0.18 | 0.43 | 0.34 | 0.50 | 0.18 |
| CaO | 0.05 | 0.00 | 0.00 | 0.06 | 0.10 | 0.00 | 0.00 | 0.00 | 0.02 | 0.00 |
| $Na_2O$ | 0.09 | 0.00 | 0.00 | 0.05 | 0.04 | 0.00 | 0.32 | 0.00 | 0.12 | 0.00 |
| $K_2O$ | 9.69 | 9.96 | 9.89 | 9.91 | 9.95 | 9.82 | 9.10 | 9.32 | 9.90 | 9.82 |
| F | 0.610 | 0.820 | 2.496 | 1.592 | 0.972 | 2.988 | 1.873 | 2.51 | 1.87 | 1.98 |
| $H_2O$** | 3.306 | 3.676 | 2.925 | 3.321 | 3.596 | 2.621 | 3.175 | 2.887 | 3.175 | 3.15 |
| Total | 100.93 | 100.88 | 100.79 | 100.03 | 100.82 | 99.66 | 100.79 | 99.72 | 100.10 | 100.39 |
| numbers of ions on the basis of 24 (O, OH, F) | | | | | | | | | | |
| Si | 5.977 | 5.868 | 6.041 | 6.027 | 5.780 | 6.058 | 5.906 | 6.104 | 6.049 | 6.124 |
| $Al^{iv}$ | 2.023 | 2.132 | 1.959 | 1.973 | 2.220 | 1.942 | 2.094 | 1.896 | 1.951 | 1.876 |
| $Al^{vi}$ | 0.565 | 0.702 | 0.558 | 0.193 | 0.684 | 0.447 | 0.122 | 0.604 | 0.208 | 0.980 |
| Ti | 0.000 | 0.000 | 0.024 | 0.000 | 0.089 | 0.007 | 0.000 | 0.000 | 0.000 | 0.007 |
| $Fe^{+2}$ | 2.047 | 2.059 | 1.722 | 1.681 | 2.059 | 1.897 | 1.791 | 1.798 | 1.451 | 1.871 |
| Mg | 3.106 | 2.933 | 3.363 | 4.044 | 2.818 | 3.438 | 4.118 | 3.328 | 4.207 | 3.392 |
| Mn | 0.080 | 0.083 | 0.089 | 0.026 | 0.070 | 0.023 | 0.054 | 0.042 | 0.062 | 0.022 |
| Ca | 0.007 | 0.000 | 0.000 | 0.009 | 0.016 | 0.000 | 0.000 | 0.000 | 0.003 | 0.000 |
| Na | 0.027 | 0.000 | 0.000 | 0.014 | 0.011 | 0.000 | 0.092 | 0.000 | 0.034 | 0.000 |
| K | 1.821 | 1.874 | 1.840 | 1.860 | 1.876 | 1.861 | 1.713 | 1.749 | 1.847 | 1.836 |
| F | 0.750 | 0.383 | 1.152 | 0.741 | 0.454 | 1.403 | 0.874 | 1.167 | 0.962 | 0.918 |
| OH | 3.242 | 3.617 | 2.848 | 3.259 | 3.546 | 2.597 | 3.126 | 2.833 | 3.038 | 3.082 |
| 100Mg: (Mg+Fe) | 60.27 | 58.73 | 66.13 | 70.63 | 58.19 | 64.45 | 69.66 | 64.91 | 74.39 | 64.43 |

* Total iron reported as FeO. ** $H_2O$ was calculated assuming F+OH=4

Sample numbers and localities

1) DDH-U43-19J, at 81'; 2) DDH-U64-17A, at 208'; 3) DDH-U68, at 190';
4) 74-UG7, Station 108, 1201-092 East Drift; 5) 74-UG25; 1103-080 West Ramp;
6) ZKSP-74-4, 1153-071 North Ramp; 7) 74-UG-21, Near Station 96, 1201-092 East Drift;
8) 74-UG-28, Near Station 78, 1201-092 East Drift; 9) 74-UG-11, Near Station 94, 1201-092 East Drift; 10) G1, Near Station 75, 1201-114 South Cross-Cut.

racy of energy-dispersive analysis was checked against a sample of garnet (S. 76) which was analyzed before and after each unknown; analyses were rejected if the results for this standard differed by more than 1.0 percent from the accepted values.

Fluorine was determined by wavelength-dispersive microprobe analysis, using an accelerating voltage of 10 kV, a beam current of $0.64\times 10^{-7}$A, a beam diameter of 20-40$\mu$m, and a KAP detector crystal. At least ten analyses, each with a 20 sec. counting period, were made on a standard fluorite specimen prior to each set of unknown analyses, and at 30 min. intervals thereafter. Errors due to the volatility of the fluorite standard were minimized by analyzing different areas of the mount each 20-sec. run. A minimum of five 200-secs. spot analyses was made for each silicate grain, the current being continuously monitored throughout.

The analytical data, collected on paper tape, were corrected for drift, background, dead-time, mass-absorption, atomic-number and fluorescence effects using the correction programs TAPEEMX and TAPEEMX2 developed by M. I. Corlett (priv. comm.).

Bourne (1974) has estimated, from counting statistics, that the uncertainty in the microprobe fluorine determination is *ca.* ± 5% of the amount present. However, the strong and variable absorption of the X-rays emitted by fluorine by the conductive carbon coating on the microprobe mount would tend to increase the absolute uncertainty. Allen (1976) has estimated that, for an accelerating potential of 10 kV, a 300Å difference in film thickness between standard and sample mounts would generate a 7% error in fluorine analysis. He therefore estimated a minimum uncertainty of ± 10% of the amount of fluorine present in a silicate mineral. As a check on the microprobe fluorine analyses, six specimens of amphibole and mica (including two duplicates) were submitted to Bondar-Clegg Co. Ltd. for ion-specific-electrode analysis. Their results were considered reproducible to within ± 0.1 wt.%F. The fluorine contents found by microprobe analysis were from 0.2 to 0.4 wt.% higher than those obtained by electrode analysis. This is probably due to impurities in the separates submitted for electrode analysis, and encourages acceptance of the microprobe data for fluorine. In the present discussion, only the microprobe F determinations will be considered.

Chlorine was found to be present in amounts

below the limit of detection of the energy-dispersive microprobe method (*i.e.*, below *ca.* 0.2 wt.%), in all amphiboles and micas.

*Mineral compositions*

In the calculations of the amphibole and mica chemical formulae, presented in Tables 1 and 2, all iron was assumed to be in the $Fe^{2+}$ state, and initially no samples were subjected to ferrous-iron determination. Whereas this is probably a reasonable procedure for the amphiboles, it requires justification in the case of the micas.

Low $Fe^{3+}$ contents for these minerals would be suggested by the relatively low oxygen fugacities which may be assumed to have prevailed during crystallization of the Fe-rich skarn assemblages. Although graphite is not present in the pyrrhotite-rich E–Zone orebody, magnetite is also absent. In the calculation of the compositions of Fe– and Mn–rich garnets of the earlier clinopyroxene–garnet skarn (Zaw 1976), the $R^{3+}$ sites were first filled, and stoichiometric considerations then indicated that, whereas almandine is present in amounts up to 19.4 mole %, andradite does not exceed 9.8 %. Thus, relatively reducing conditions are implied.

A more precise estimate of the maximum value of log $f(O)_2$ may be made from the thermochemical data presented by Holland (1965) for the system Fe–S–O at 400°C, on the assumption that the hexagonal pyrrhotite intergrown with the biotite retained its original composition during cooling of the orebody. The pyrrhotite is a major constituent of the biotite skarn, and is not associated with either magnetite or pyrite. Reaction with the mica may indeeed have occurred, but there is no textural or compositional evidence for this. The pyrrhotite is relatively homogeneous, with a mean composition of 47.61 at.% FeS. At 415°C, this composition would imply a value of log $f(S)_2$ of –8.5, (Toulmin & Barton 1964), yielding a maximum value for log $f(O)_2$ of –27.4 for pyrrhotite stability. Thus, oxygen fugacity during the formation of the biotite skarn probably did not greatly exceed that of the QFM buffer (log $f(O_2)$ *ca.* –29.37 at 688°K and 1000 bars: Eugster 1957). The data of Wones & Eugster (1965) suggest that the $Fe^{3+}/(Fe^{2+}+Fe^{3+})$ ratio of the biotite is less than *ca.* 0.05. A range for this ratio of between 0.05 and <0.02 would be inferred if the biotite crystallized under oxygen fugacities between those of the QFM and C–CH buffers (Wones & Eugster 1965).

Despite the above inference of a low ferric iron content in the micas, selected wet chemical determinations of total and ferrous iron contents were undertaken, in view of the apparent correlation of biotite color with $Fe^{3+}$ and $TiO_2$ contents (Deer *et al.* 1962a). Previous studies indicated that high $Fe^{3+}$ contents produce green colors in biotite, whereas high Ti causes a brown coloration. The lack of correlation between titanium content and E-Zone biotite color (Table 2) left open the possibility that the greenish specimens are richer in $Fe^{3+}$ than the others. Thus, two coarse-grained mica concentrates, one green and one brown, were carefully prepared and analyzed by the colorimetric method of Wilson (1960), employing an oxidimetric standard recommended by Caraway & Oesper (1947). In each case, very low contents of ferric iron were detected; $Fe^{3+}/(Fe^{2+}+Fe^{3+})$ ratios of 0.035 and 0.038 were estimated for the green and brown micas, respectively. Unfortunately, it is not possible to determine $Fe^{2+}$ in the specimens studied by electron microprobe. However, on the basis of these limited data, we tentatively conclude that $Fe^{3+}$ is very low in the E-Zone micas and, therefore, that the contents of "oxybiotite" are comparably low.

Interestingly, in experimental studies of fluorite-hydroxyl exchange in biotites, Munoz & Ludington (1974) assumed an oxybiotite content of 15 mole % when calculating the F:OH ratios of their micas. They inferred that their biotites, synthesized under conditions intermediate between the NNO and C–CH oxygen buffers, probably contained between 10 and 25 mole % oxybiotite. However, they detected no systematic differences in distribution coefficients that could be related to differences in $f(O_2)$. In the present study, the OH contents and F:OH ratios have been calculated directly from the determined fluorine contents, making no allowance for either O or Cl in the structure.

Amphibole and mica structural formulae (Tables 1 and 2) were calculated using either a program written by P. L. Roeder or the CHEMFORM Fortran program by J. M. Allen (priv. comm.). The formulae were first calculated on an OH– and F–free basis, and OH was then allotted such that OH+F equalled the stoichiometric amounts in the formulae. Weight % $H_2O$ was then calculated from the amount of OH in the formula. In allotting ions to sites in both minerals, it was assumed that the tetrahedral positions were filled with Si and Al, and the excess of Al was then ascribed to the octahedral positions (*cf.*, Deer et al. 1962a). Na in the amphiboles was distributed so as to fill first the *M*(4) position (Papike et al. 1969).

*Calciferous amphiboles*

The electron microprobe analyses presented in

Table 1 show that the E-Zone amphiboles display a fairly wide range in $Mg/(Mg+Fe^{2+})$ ratio, and are calciferous (Leake 1968) in that the CaO in their half unit cells (O=24) exceeds 1.5. There is substantial substitution of K and Na for Ca, the total of these elements remaining close to 2.0 in the structural formula.

In Figure 2, the nine analyzed amphiboles have been plotted on the Ca-amphibole diagram of Leake (1968); Mn and $Fe^{3+}$ have not been considered. The Mg and Fe end-members tremolite and ferroactinolite proposed by Deer *et al.* (1962b) have been retained, but the boundaries of the actinolite field are modified. It will be seen that eight of the samples, including both pale and dark varieties, plot within the

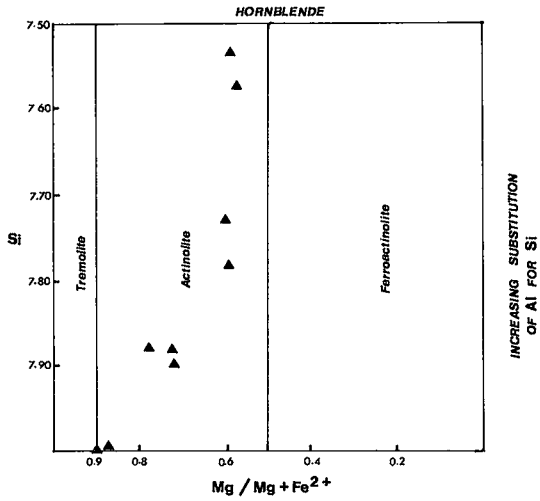


FIG. 2. Compositional plot for E–Zone skarn Ca-amphiboles (after Leake 1968).

actinolite field, only one falling at the tremolite–actinolite boundary. Although there is a wide variation in the tetrahedral aluminum content, the compositions do not overlap onto the hornblende field. $Al^{IV}$ and $Mg/(Mg+Fe^{2+})$ display a broad, inverse relationship. Octahedral aluminum attains 0.548 atoms in the formulae, and shows a very crude *positive* correlation with Mg content. However, the nine samples could also be regarded as comprising two populations in this context: one has high Mg and varies widely in $Al^{VI}$ (from 0.082 to 0.548), and the other has higher Fe and uniformly low $Al^{VI}$ (from 0.003-0.162).

The E-Zone amphiboles display relatively high MnO contents, ranging up to 1.23 wt.%, in keeping with the overall enrichment of manganese in the E-Zone skarns (Zaw 1976).

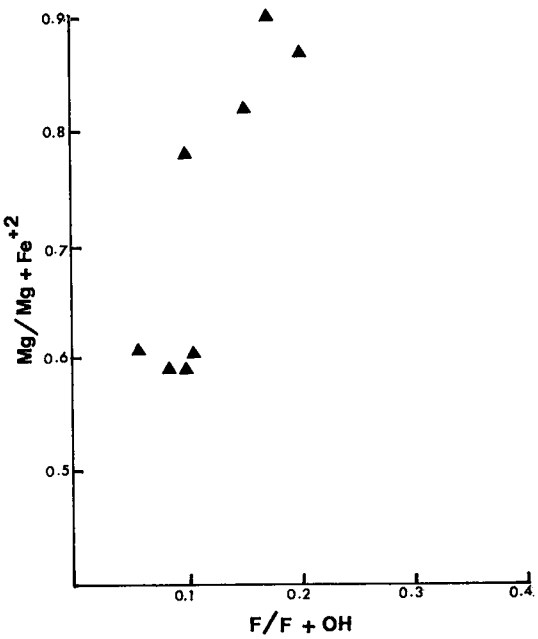


FIG. 3. Relationships between Mg/(Mg+Fe) and F/(OH+F) ratios, E–Zone skarn amphiboles.

Fluorine exhibits a relatively well-defined correlation with $Mg/(Mg+Fe^{2+})$ ratio (Fig. 3), a feature that has been reported by several other investigators (*e.g.*, Ekström 1972; Allen 1976); biotites also show this feature (see below). Fluorine was not determined in sample #4, and the structural formula was calculated assuming it to be absent; however, the Mg/Fe ratio implies a relatively high F content (see below). Ramberg (1952) and Cameron & Gibbs (1973) proposed that the relative enrichment of fluorine in magnesian amphiboles reflects the formation of stronger Mg–F than $Fe^{2+}$–F bonds. Cameron (1971; *in* Rosenberg & Foit 1977) concluded that, in synthetic fluor-richterite, $Fe^{2+}$ avoids bonds with $F^-$ by concentrating in the *M*2 sites, where the coordinating anions are all $O^{2-}$, rather than in the *M*1 or *M*3 sites, where $F^-$ occurs. Rosenberg & Foit (1977) have recently provided a qualitative crystal-field theory explanation for $Fe^{2+}$–F avoidance in hydrous silicates.

Troll & Gilbert (1972) carried out hydrothermal experiments on fluoride:hydroxyl exchange between tremolite and an aqueous fluid, under 1–2 Kbar pressure and between 600° and 850°C. They found that, under the oxygen fugacity of the QFM buffer, tremolite has the composition $F_{55.00}OH_{43.00}$ at 700°C and at 1 Kbar. However, they encountered considerable difficulties owing to sluggish reaction rates, and

their data cannot be extrapolated to the temperatures of formation of the E–Zone amphibole skarn, nor to the Fe-rich compositions of E-Zone actinolites. Relative F:OH exchange characteristics of Ca-amphiboles and micas will be discussed below.

*Micas*

The composition of ten analyzed skarn micas from the E-Zone orebody are plotted in Figures 4 and 5 (after Deer *et al.* 1962a) in terms of the phlogopite, annite, eastonite and siderophyllite end-members, omitting from consideration the MnO, $TiO_2$, CaO and $Na_2O$ contents. From Table 2, it is evident that, despite the wide color variations of these micas, the $K_2O$ contents are uniformly high, and the minerals are clearly unaltered. Whereas there is some tendency for the brown micas to have lower $Mg/(Mg+Fe^{2+})$ ratios than the green, there is considerable compositional overlap between the two varieties. The micas straddle the boundary between biotite and phlogopite proposed by Deer *et al.* (1962a), but herein they will be referred to as biotites.

The biotites display a wide variation in $Al^{VI}$ (0.122–0.980), but a more restricted range in $Al^{IV}$ (1.876–2.220). Thus, whereas they lie close to the phlogopite–annite join (Fig. 4), the variation in octahedral aluminum suggests that they are best described as members of the phlogopite–siderophyllite "series"; this possibly oversimplified assignment will be used in the following discussion of fluorine:hydroxyl exchange. There is no systematic relationship between $Al^{VI}$ and $Mg/(Mg+Fe^{2+})$ or $Mg/(Mg+Fe^{2+}+Mn)$ (*cf.*, Guidotti *et al.* 1975).

From Fig. 6, it is evident that $F/(OH+F)$ and $Mg/(Mg+Fe^{2+})$ exhibit a broadly sympathetic relationship in these biotites, comparable to that shown by the actinolites. Munoz & Ludington (1974) have shown that more magnesian biotites tend to have higher *maximum* F contents. Jacobs & Parry (1976) and Allen (1976), among others, have recently presented analytical data demonstrating this trend. The data points in this diagram fall well within the field outlined by Munoz

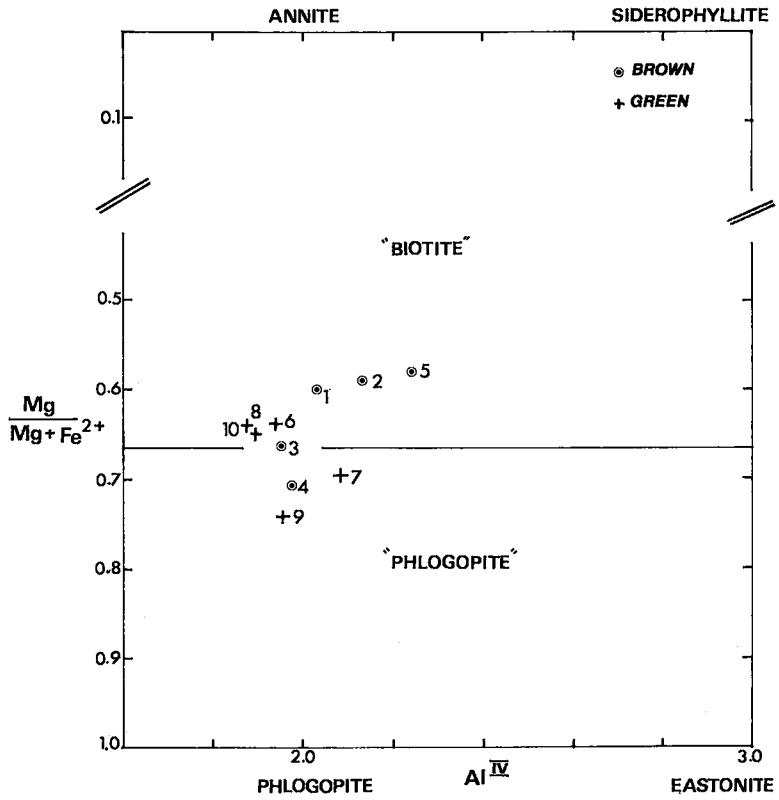


FIG. 4. $Mg/(Mg+Fe)$ *vs.* $Al^{IV}$ plot for E–Zone skarn micas (after Deer *et al.* 1962a).

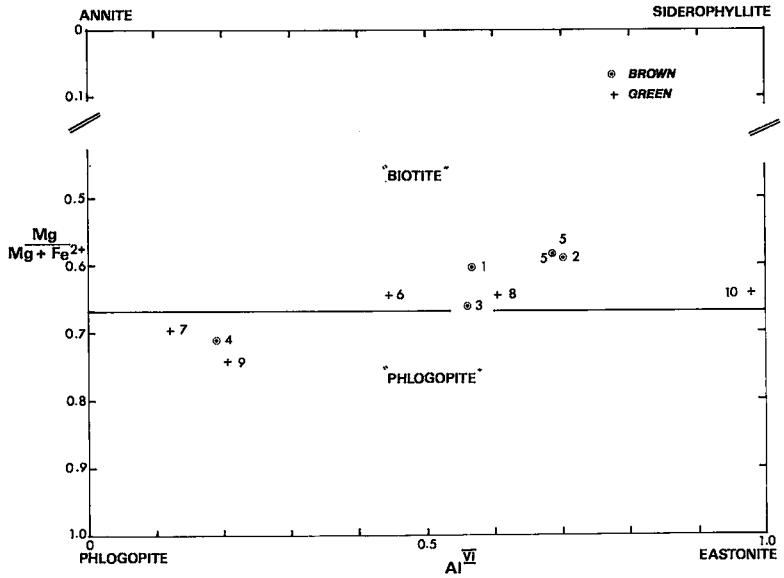


FIG. 5. Mg/(Mg+Fe) *vs.* $Al^{VI}$ plot for E–Zone skarn micas.

& Ludington (1974) in their compilation of previously published data for biotites from different geological environments; the Cantung hydrothermal micas are thus not significantly enriched in fluorine for their magnesium contents.

## FLUORIDE:HYDROXYL EXCHANGE BETWEEN BIOTITES AND FLUID

Munoz & Ludington (1974) measured fluoride:hydroxyl distribution coefficients in syn-

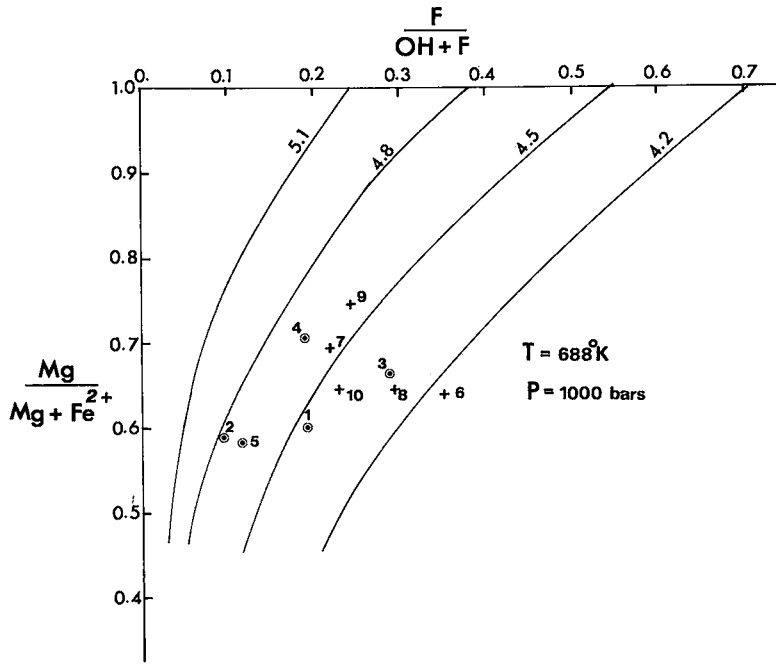


FIG. 6. Relationship between Mg/(Mg+Fe) and F/(OH+F) ratios, E–Zone skarn biotites. Contours are for log $f(H_2O)/f(HF)$ for the fluid coexisting with phlogopite–siderophyllite solid solutions at 688°K and 1000 bars.

thetic phlogopite, annite and siderophyllite, using the fluorine buffer technique, according to the reaction: ½hydroxybiotite + HF = ½fluor-biotite + $H_2O$. Hydrothermal experiments were carried out between 454 and 738°C (most above 550°C) at 1–2 Kbars. The F/OH ratios of equilibrated biotites were calculated from indirect spectrophotometric fluorine analysis, assuming 15 mole % "oxybiotite" in the mica structure.

It was demonstrated that, at a particular $f(H_2O):f(HF)$ ratio in the gas (fluid) phase, the F:OH ratio of the biotite is markedly affected by temperature, by the cationic ratios of the mineral ($Mg/(Mg+Fe^{2+})$) and, to a lesser degree, by the confining fluid pressure. Subsequently, Ludington & Munoz (1975) revised the original exchange equations thus:

(1) for phlogopite, $\log K = \frac{2100}{T} + 1.523 + \frac{0.0093\ (P-1)}{T}$;

(2) for annite, $\log K = \frac{2100}{T} + 0.416 + \frac{0.0181\ (P-1)}{T}$;

(3) for siderophyllite, $\log K = \frac{2100}{T} + 0.079 + \frac{0.0107\ (P-1)}{T}$,

where T is in K, and P is in bars.

Ludington & Munoz found that, if octahedral mixing properties are near-ideal, the free energy of fluoride: hydroxyl exchange is a linear function of cationic compositions between the above end-members. Thus, if the Cantung E–Zone biotites are regarded as intermediate in composition between plogopite and siderophyllite, $\log K = \frac{2100}{T} + 0.079 + \frac{0.0107\ (P-1)}{T} + (X_{Mg})^{\frac{3}{2}} \left[1.444 - \frac{0.0014\ (P-1)}{T}\right]$ (eq. 4), where $X_{Mg}$ represents the mole fraction of (OH, F) phlogopite in the biotite. The effects of additional cations on the exchange have been neglected; Ludington & Munoz (1975) infer that whereas Li (probably very minor in the Cantung biotites) may have a large effect on F-OH exchange, Mn and Na probably exert only a minor influence.

The temperatures and confining pressures of hydrothermal biotite crystallization are relatively well-defined: mean values of 415°C (688°K) and 1000 bars are here assumed. Thus, from equation 4 above, $\log K = 3.146 + 1.442\ (X_{Mg})^{\frac{3}{2}}$ (eq. 5).

Now, assuming ideal mixing of F and OH, $\log K = \log \left(\frac{X_{Fbi}}{X_{OHbi}}\right)^{biotite} + \log \left(\frac{f(H_2O)}{f(HF)}\right)^{fluid}$ (eq. 6), where $X_{Fbi}$ and $X_{OHbi}$ are mole % fluor-biotite and hydroxy-biotite, respectively. Therefore, the fugacity ratio $f(H_2O)/f(HF)$ in the fluids responsible for formation of the micaceous skarns at Cantung may be estimated from:

$\log [f(H_2O)/f(HF)]^{fluid} = 3.146 + 1.442\ (X_{Mg}^{bi})^{\frac{3}{2}} - \log (X_F/X_{OH})^{bi}$ (eq. 7)

Values of $X_{Mg}$ ($Mg/(Mg+Fe^{2+})$) and fluoride: hydroxyl ratios for the E-Zone biotites and the calculated values for the term $\log f(H_2O)/f(HF)$ for the coexisting fluid phase are presented in Table 3. The log fugacity ratios are seen to vary from 4.16 to 4.77, a relatively narrow spread of values. In Fig. 6, the mica compositions are plotted in terms of $X_{Mg}$ and F/(OH+F), with contours for $\log f(H_2O)/f(HF)^{fluid}$ for phlogopite-siderophyllite solid solutions at 415°C and 1000 bars (*cf.*, Fig. 7 of Munoz & Ludington 1974). From this plot, it could be concluded that all biotite in the E-Zone skarn crystallized in equilibrium with a fluid phase with a log fugacity ratio of 4.5±0.3. This would imply a relatively consistent solution fugacity ratio. However, in comparison with the comparable data presented by Munoz & Ludington (1974), it could be inferred that the distribution of data points across the iso-fugacity ratio contours indicates that the fugacity ratio varied significantly during ore formation, or that the *ca.* 100°C temperature range found in the fluid-inclusion-homogenization runs is real, and responsible for at least some of the apparent fugacity-ratio variation. This question cannot be resolved at present.

TABLE 3. SELECTED COMPOSITIONAL DATA FOR E-ZONE BIOTITES AND CALCULATED VALUES FOR LOG ($\underline{f}(H_2O)/\underline{f}(HF)$) IN THE COEXISTING FLUID.

| Sample No. | $(Mg/Mg+Fe)^{biotite}$ | $(X_F/X_{OH})^{biotite}$ | $Log(\underline{f}(H_2O)/\underline{f}(HF))^{gas}$ |
|---|---|---|---|
| 1 | 0.603 | 0.231 | 4.46 |
| 2 | 0.587 | 0.106 | 4.77 |
| 3 | 0.661 | 0.405 | 4.31 |
| 4 | 0.706 | 0.227 | 4.64 |
| 5 | 0.582 | 0.128 | 4.68 |
| 6 | 0.645 | 0.540 | 4.16 |
| 7 | 0.697 | 0.280 | 4.54 |
| 8 | 0.649 | 0.376 | 4.33 |
| 9 | 0.744 | 0.372 | 4.50 |
| 10 | 0.644 | 0.298 | 4.42 |

The limitations of the above estimates should be emphasized. Munoz & Ludington (1974) proposed an uncertainty of ±0.2 in their original log $K$ values for the biotite end-member compositions, between 500°C and 700°C. This was derived mainly from uncertainties in the free energies of the fluorine buffer phases, but also from possible inaccuracies in the estimation of F:OH ratios in the micas and from the method used for estimation of the AFSQ buffer–fluid data from calculated QFM data. The Cantung assemblages formed below 500°C, and therefore would probably be subject to greater uncertainties. However, Munoz & Ludington (1974) observe that *relative* changes in $f(H_2O)/f(HF)$ are better estimated from F:OH exchange data than are absolute values.

The fugacity of HF in the Cantung ore-forming fluid may be estimated on the assumption that the latter contained only HF and $H_2O$. At a pressure of 1000 bars and at 415°C, pure water has a fugacity of 285 bars (Burnham *et al.* 1969). Thus, the fugacity of HF was approximately 0.009 bars. On this basis, it is concluded that the ore solutions which generated the biotitic skarns possessed a very low HF fugacity, and that this was almost certainly exceeded by the fugacities of $CO_2$ and of Cl gas species.

Comparison of Figs. 3 and 6 reveals that, in general, the E-Zone actinolites contain significantly less fluorine than the later-deposited biotites, although it is of interest to note that the more Fe-rich amphiboles display F/(OH+F) ratios similar to those of biotites with similar Mg/Fe ratios.

The E-Zone assemblages unfortunately do not provide close constraints on the relative F:OH exchange characteristics of actinolite and biotite because the amphiboles were deposited at *ca.* 20°C higher than the micas and, more critically, because it cannot be assumed that the $f(H_2O)/f(HF)$ ratio in the ore-forming fluid remained constant throughout these two skarnification stages.

## Comparison of Magmatic and Hydrothermal Biotites

Numerous authors (*e.g.*, Moore & Czamanske 1973, Beane 1974, Jacobs & Parry 1976) have drawn attention to the fact that hydrothermal biotites from porphyry copper deposits tend to be more magnesian than magmatic biotites from the host stocks. It would be of interest to determine whether such a relationship holds for the contact metasomatic mineralization at Cantung. Further, it should be possible, from the composition of the magmatic biotite, to estimate the HF fugacity of the last fluid phase which migrated through the upper part of a pluton, assuming that equilibrium was attained betwen mica and fluid at the post-magmatic stage.

TABLE 4. ELECTRON MICROPROBE ANALYSES AND STRUCTURAL FORMULAE OF BIOTITES FROM THE CIRCULAR STOCK, CANTUNG.

| Weight % | 1 | 2 | 3 | 4 |
|---|---|---|---|---|
| $SiO_2$ | 40.82 | 39.48 | 40.25 | 38.32 |
| $Al_2O_3$ | 21.07 | 20.37 | 20.22 | 19.15 |
| $TiO_2$ | 3.13 | 3.59 | 2.93 | 3.06 |
| [1]FeO | 14.42 | 15.45 | 15.22 | 20.97 |
| MgO | 7.08 | 6.83 | 7.36 | 4.89 |
| MnO | 0.38 | 0.22 | 0.38 | 0.07 |
| CaO | 0.00 | 0.00 | 0.00 | 0.00 |
| $Na_2O$ | 0.00 | 0.11 | 0.49 | 0.11 |
| $K_2O$ | 9.24 | 9.04 | 9.04 | 9.53 |
| F | 0.42 | 0.35 | 0.30 | 0.41 |
| [2]$H_2O$ | 3.96 | 3.91 | 4.02 | 3.79 |
| Total | 100.35 | 99.20 | 100.21 | 100.13 |
| | numbers of ions on the basis of 24 (O, OH, F) | | | |
| Si | 5.892 | 5.809 | 5.799 | 5.768 |
| $Al^{iv}$ | 2.108 | 2.191 | 2.201 | 2.232 |
| $Al^{vi}$ | 1.476 | 1.341 | 1.403 | 1.165 |
| Ti | 0.340 | 0.397 | 0.318 | 0.346 |
| $Fe^{+2}$ | 1.741 | 1.901 | 1.834 | 2.639 |
| Mg | 1.524 | 1.497 | 1.580 | 1.097 |
| Mn | 0.046 | 0.028 | 0.046 | 0.009 |
| Ca | 0.000 | 0.000 | 0.000 | 0.000 |
| Na | 0.000 | 0.031 | 0.137 | 0.032 |
| K | 1.702 | 1.697 | 1.663 | 1.830 |
| F | 0.191 | 0.163 | 0.137 | 0.195 |
| OH | 3.809 | 3.837 | 3.863 | 3.805 |
| 100Mg:(Mg:Fe) | 46.00 | 44.00 | 46.00 | 29.00 |

Sample numbers and localities: 1) CS-7; 2) CS-8; 3) CT-AHC; 4) CT-AHC-8; all samples collected from the Circular Stock.

[1]Total iron reported as FeO.

[2]$H_2O$ was calculated assuming F+OH ≡ 4.

Four fresh biotites from surface samples of the Circular Stock, located 1.6 km north of the E–Zone orebody, were analyzed (Table 4). Biotites in the Mine Stock immediately underlying the E-Zone are partly sericitized, and were not studied.

It is evident that the magmatic biotites are markedly enriched in Fe relative to those in the skarns, in accordance with the observations of previous investigators of the porphyry environment, although they are not depleted in Si, Al and K. Indeed, the magmatic biotites are seen to be extremely aluminous; whereas $Al^{IV}$ ranges from 2.108 to 2.232, only slightly higher than that in the skarn micas, $Al^{VI}$ attains levels of 1.341–1.476 ions. Few comparably aluminous biotites are recorded by Deer *et al.* (1962a); these are from metamorphic rather than plutonic rocks. Guidotti *et al.* (1975) present numerous analyses of highly aluminous biotites from metamorphic and granitoid rocks, but in these, the high $Al_2O_3$ contents are balanced by low $SiO_2$, thereby limiting the $Al^{VI}$ contents to 1 in all

cases. In contrast, the $SiO_2$ contents of the Circular Stock biotites are uniformly high. Further, these micas plot close to the $(Al^{VI} + Ti^{4+})$ and $(Fe^{2+} + Mn^{2+})$ limits of the compositional field in the *Y*-position cationic plot presented by Neilson & Haynes (1973) for biotites from numerous calc-alkaline plutonic rocks. No immediate explanation for these clearly unusual biotite compositions can be offered. The bulk composition of the Circular Stock quartz monzonite (Zaw 1976) is not unusual, and there is no microscopic evidence (*e.g.*, occurrence of aluminosilicate minerals) which would reveal the incorporation of pelitic rocks in the magma.

The number of ions in octahedral sites is very low in these biotites, not exceeding 5.26 per formula unit. Thus, in the plot proposed by Deer *et al.* (1962a) to relate the dioctahedral and trioctahedral (Fe-free) micas (their Fig. 14, Si *vs.* total *Y*-position cations), the Cantung micas fall very close to the limit of the field of trioctahedral micas.

The magmatic biotites display a rather uniform fluorine content (0.30–0.42 wt. %), markedly lower than that in the skarn micas. Although the biotites in the stock fall outside of the phlogopite–eastonite–siderophyllite–annite compositional field, it will here be assumed that they, like the skarn micas, may be assigned to the phlogopite–siderophyllite series. It is further assumed that they last equilibrated with a hydrothermal fluid at a temperature of 550°C, slightly higher than that found for the early clinopyroxene–garnet skarn stage in the E-Zone. On this basis, the $X_{Mg}$ and $X_F/X_{OH}$ ratios of the biotites suggest that they equilibrated with an aqueous fluid with log $f(H_2O)/f(HF)$ of between 4.16 (spec. 4) and 4.46 (spec. 3). This range is essentially identical to that calculated for the biotitic-skarn stage of mineralization. If it can be assumed that the Circular Stock biotites interacted with the fluids responsible for the formation of the small, non-economic bodies of clinopyroxene–garnet exoskarn which occur adjacent to the pluton, it may very tentatively be inferred that, in the main Cantung orebodies, $f$(HF) remained sensibly constant during the successive formation of the clinopyroxene–garnet, actinolite and biotite skarns.

## Comparison with Other Hydrothermal Ore Deposits

In a broader context, a tentative comparison may be made between the $f$(HF) values inferred for the Cantung E–Zone skarn with those indicated by analyses of hydrous silicates from other skarn and porphyry deposits. There are, however, few comparable analytical studies of hydrothermal biotites and amphiboles, and few published estimates of HF fugacities in such deposits. In particular, no data for other scheelite skarns have been located in a review of the literature.

In his detailed study of the Tsumo Cu–Zn–Pb skarn deposit, Japan, Shimazaki (1968) presents complete analyses for one tremolite and two phlogopites with high fluorine contents (2.61 and 3.43, 4.38 wt.%, respectively). Chondrodite coexists with both minerals, consistent with a relatively F-rich environment. If it is assumed that the highly magnesian micas described by Shimazaki conform to the phlogopite–siderophyllite join and, more importantly, that they crystallized under P–T conditions similar to those in the E–Zone, their compositions would indicate log $f(H_2O)/f(HF)$ values of $4.5\pm0.1$. These are remarkably similar to the conditions estimated for skarn mineralization in the Cantung E–Zone.

Haynes & Clark (1972) found that hydrothermal magnesian biotite from the large Boquerón Chañar skarn magnetite deposit, Atacama, Chile, very probably of contact metasomatic origin, is strongly enriched in both F and Cl (2.32 and 1.12 wt.%, respectively). The fluorine content is similar to that of the Cantung micas, whereas the high chlorine content implies an unusually high salinity for the ore-forming fluid.

Geijer (1961) has reported fluorine concentrations for amphiboles from several Swedish contact- and regional ("reaction") skarn deposits. His analysis of anthophyllite from the Kaveltorp Pb–Zn–Cu contact skarn (1.15%F) suggests formation conditions similar to those at Cantung, as do the fluorine concentrations (0.23–2.34%) for several contact metasomatic magnetite ores (although the F contents are widely variable).

Published data for fluorine contents, and less commonly, for F/(OH+F) and Mg/(Mg+Fe) ratios of hydrothermal biotites from porphyry copper deposits (*e.g.*, Kesler *et al.* 1975; Jacobs & Parry 1976; Haynes 1975) reveal generally lower fluorine levels than in skarn micas, suggesting that $f$(HF) is even less in the porphyry than the contact-metasomatic-mineralization environment. However, some values given by Kesler *et al.* (1975) for Bingham, Utah imply HF fugacities similar to those at Cantung and Tsumo.

Burt (1972) has suggested that the predominance of wolframite (actually, ferberite) rather than scheelite as the tungsten mineral in quartz-vein deposits associated with greisens, and its

almost complete absence in the majority of skarns, is not a direct reflection of the relative activities of Fe and Ca in these two settings. On the basis of a schematic diagram relating the chemical potentials of $CO_2$ and F (expressed as $F_2O_{-1}$), in which decarbonation and defluoridation mineral reactions in the system Ca–Fe–W–O–C–F are portrayed, he concluded that the scheelite–calcite and ferberite–fluorite assemblages are stable in two widely separated fields characterized by high $\mu CO_2$– low $\mu F_2O_{-1}$ and low $\mu CO_2$–high $\mu F_2O_{-1}$, respectively. Thus, the fugacity ratio $f(HF)/f(CO_2)$ would determine which tungstate mineral would be deposited.

In broad terms, the low HF fugacity estimated in the present study for the Cantung skarns is consistent with Burt's hypothesis. However, it remains to be shown that the $f(HF)/f(CO_2)$ at Cantung and in other scheelite skarns was indeed lower than that prevailing during the formation of the majority of wolframite–quartz veins, many of which (*e.g.*, Panasqueira, Portugal) contain considerably more calcite (or other carbonates) than fluorite.

## Mechanism of Scheelite Transport and Deposition

The very low HF fugacity herein calculated for the hydrothermal solutions in the Cantung E–Zone, an orebody representing a major crustal concentration of fluorine, lends no direct support to the efficacy of aqueous fluoride species in the transport of scheelite. However, Foster (1977) has experimentally demonstrated that over the temperature range represented by many scheelite deposits, this mineral is significantly soluble in pure water, but its solubility is greatly enhanced in 1*M* KCl solutions in which $P(H_2O)$ is buffered by the assemblage quartz–K feldspar–muscovite. Moreover, it was shown that scheelite solubility in such dilute solutions at $P(H_2O) = 1000$ bars (a pressure comparable to that at Cantung) decreases considerably on cooling from 500°C (500 ppm) to 300°C (100 ppm). Scheelite solubility is dependent upon P(HCl). Foster concludes that molecular $H_2WO_4$ is probably the dominant W species in such near-critical conditions and at higher temperature, but that complexes involving HCl and KCl ligands may also contribute to solubility of tungsten.

Foster elegantly applies his experimental data to explain the association of scheelite and native gold in quartz-vein deposits in granite–greenstone terrains, but states that these relationships should not be extrapolated to the contact-skarn setting, where abrupt changes in solution pH may be expected to promote scheelite precipitation. However, at Cantung, emplacement of the biotite exoskarn was accompanied by the formation of scheelite-bearing quartz veins in the underlying pluton. The temperature of scheelite deposition in these values (mean 405°C: Zaw 1976) overlapped extensively with that of the skarn. Thus, the two juxtaposed types of mineralization are considered to represent differing segments of a single, spatially continuous hydrothermal circulation system involving dilute brines, as shown by fluid-inclusion-freezing data.

In the quartz veins, scheelite coexists with microcline and muscovite; therefore, depositional conditions were directly comparable to those in Foster's experimental runs. Thus, solutions migrating upward through the roof zone of the Mine Stock were in a P–T–*X* field in which scheelite solubility is markedly affected by decreasing temperature. Under these conditions, it is perhaps surprising that the quartz veins at Cantung are not more intensely mineralized. It is inferred that the solutions thereafter migrated from the stock into the Ore Limestone marbles, where an abrupt increase in pH caused a massive precipitation of scheelite.

## Acknowledgements

Canada Tungsten Mining Corporation have given permission for publication of this paper, and generously provided the authors with much logistical assistance in the field. Messrs. L. D'Aigle, B. K. Bowen, and N. Cawthorn, of the Canada Tungsten Geological Department, are thanked for their practical assistance at the mine, and for many useful discussions. At Queen's University, Drs. P. L. Roeder, M. I. Corlett, and J. M. Allen provided much assistance and encouragement in the analytical studies. Emma Fernando prepared the illustrations. Zaw was supported by a post-graduate fellowship from the Training and Fellowship Programme Section, Office of Technical Cooperation, United Nations, who also provided funds to cover the costs of field and laboratory studies. Laboratory and clerical work was also supported by a National Research Council of Canada Operating Grant to A. H. Clark.

## References

Albee, A. L. & Ray, L. (1970): Correction factors for electron probe microanalysis of silicates, oxides, carbonates, phosphates and sulfates. *Anal. Chem.* 42, 1408-1414.

Allen, J. M. (1976): *Silicate-Carbonate Equilibria in Calcareous Metasediments of the Tudor Town-*

*ship Area, Ontario: A Test of the P–T–X($CO_2$) Model of Metamorphism.* Ph.D. thesis, Queen's University, Kingston, Ontario.

ANON. (1977): Canada Tungsten: record profit in 1976. *Mining J.* **288**, 377-378.

ARCHIBALD, D. A., CLARK, A. H., FARRAR, E. & ZAW, U KHIN, (1978): Potassium-argon ages of intrusion and scheelite mineralization, Cantung, Tungsten, Northwest Territories. *Can. J. Earth Sci.* (in press).

BEANE, R. E. (1974): Biotite stability in the porphyry copper environment. *Econ. Geol.* **69**, 241-256.

BENCE, A. E. & ALBEE, A. L. (1968): Empirical correction factors for the electron microanalysis of silicates and oxides. *J. Geol.* **76**, 382-403.

BLUSSON, S. L. (1968): Geology and tungsten deposits near the headwaters of Flat River, Yukon Territory and southern District of Mackenzie, Canada. *Geol. Surv. Can. Pap.* **67-22**.

BOURNE, J. H. (1974): *The Petrogenesis of the Humite Group Minerals in Regionally Metamorphosed Marbles of the Grenville Supergroup.* Ph.D. thesis, Queen's University, Kingston, Ont.

BRYZGALIN, O. V. (1958): The origin of scheelite in skarn ore deposits. *Geochem.* 297-304.

BURNHAM, C. W., HOLLOWAY, J. R. & DAVIS, N. F. (1969): Thermodynamic properties of water to 1000°C and 10,000 bars. *Geol. Soc. Amer. Spec. Pap.* **132**.

BURT, D. M. (1972): The influence of fluorine on the facies of Ca–Fe–Si skarns. *Carnegie Inst. Wash. Year Book* **71**, 443-450.

CACHAU-HERREILLAT, F. & PROUHET, J. P. (1971): The utilization of metalloids (arsenic, phosphorus, fluorine) as pathfinders for skarn tungsten deposits in the Pyrénées. *In* Geochemical Exploration, *Proc. 3rd Int. Geochem. Symp. Toronto,* 116-120.

CAMERON, M. (1971): *The Crystal Chemistry of Tremolite and Richterite: A Study of Selected Anion and Cation Substitutions.* Ph.D. thesis, Virginia Polytechnic Institute and State University, Blacksburg, Virginia.

——— & GIBBS, G. V. (1973): The crystal structure and bonding of fluor-tremolite: A comparison with hydroxyl tremolite. *Amer. Mineral.* **58**, 879-888.

CARAWAY, K. P. & OESPER, R. E. (1947): Ferrous ethylenediamine sulfate as an oxidometric standard. *J. Chem. Educ.* **24**, 235-236.

DARLING, R. (1971): Preliminary study of the distribution of minor and trace elements in biotite from quartz monzonite associated with contact-metasomatic tungsten–molybdenum–copper ore, California, U.S.A. *In* Geochemical Exploration, *Proc. 3rd Int. Geochem. Symp.* Toronto, 315-322.

DEER, W. A., HOWIE, R. A. & ZUSSMAN, J. (1962a): *Rock-Forming Minerals.* **3**. *Sheet Silicates.* Longman, London.

———, ——— & ——— (1962b): *Rock-Forming Minerals.* **2**. *Chain Silicates.* Longman, London.

EKSTRÖM, T. K. (1972): The distribution of fluorine among some coexisting minerals. *Contr. Mineral. Petrology* **34**, 192-200.

EUGSTER, H. P. (1957): Heterogeneous reactions involving oxidation and reduction at high pressures and temperatures. *J. Chem. Phys.* **26**, 1760-1761.

FOSTER, R. P. (1977): Solubility of scheelite in hydrothermal chloride solutions. *Chem. Geol.* **20**, 27-43.

GABRIELSE, H. & REESOR, J. E. (1974): The nature and setting of granitic plutons in the central and eastern parts of the Canadian Cordillera. *Pacific Geol.* **8**, 109-138.

GEIJER, P. (1961): The distribution of halogens in skarn amphiboles in Central Sweden. *Ark. Mineral. Geol.* **2**, 481-504.

GUIDOTTI, C. V., CHENEY, J. T. & CONATORE, P. D. (1975): Interrelationship between Mg/Fe ratio and octahedral Al content in biotite. *Amer. Mineral.* **60**, 849-853.

HAYNES, S. J. (1975): *Granitoid Petrochemistry, Metallogeny, and Lithospheric Plate Tectonics, Atacama Province, Chile.* Ph.D. thesis, Queen's University, Kingston, Ontario.

——— & CLARK, A. H. (1972): Distribution of chlorine and fluorine in granitoid rocks and associated ore deposits, northern Chile. *Econ. Geol.* **67**, 1005 (abstr.).

HOLLAND, H. D. (1965): Some applications of thermochemical data to problems of ore deposits. II. Mineral assemblages and the composition of ore-forming fluids. *Econ. Geol.* **60**, 1101-1166.

IVANOVA, G. F. (1966): Thermodynamic evaluation of the possibility of tungsten transport as halogen compounds. *Geochem. Int.* **3**, 964-973.

JACOBS, D. C. & PARRY, W. T. (1976): A comparison of the geochemistry of biotite from some Basin and Range stocks. *Econ. Geol.* **71**, 1029-1035.

KESLER, S. E., ISSIGONIS, M. J., BROWNLOW, A. H., DAMON, P. E., MOORE, W. J., NORTHCOTE, K. E. & PRETO, V. A. (1975): Geochemistry of biotites from mineralized and barren intrusive systems. *Econ. Geol.* **70**, 559-567.

LEAKE, B. E. (1968): A catalog of analyzed calciferous and sub-calciferous amphiboles together with their nomenclature and associated minerals. *Geol. Soc. Amer. Spec. Pap.* **98**.

LUDINGTON, S. & MUNOZ, J. L. (1975): Application of fluor-hydroxyl exchange data to natural micas. *Geol. Soc. Amer. Program Abstr.* **7**, 1179.

MOORE, W. J. & CZAMANSKE, G. K. (1973): Compositions of biotites from unaltered and altered monzonitic rocks in the Bingham mining district, Utah. *Econ. Geol.* **68**, 269-274.

MUNOZ, J. L. & LUDINGTON, S. D. (1974): Fluoride-hydroxyl exchange in biotite. *Amer. J. Sci.* **274**, 396-413.

——— & ——— (1977): Fluorine-hydroxyl exchange in synthetic muscovite and its application to muscovite–biotite assemblages. *Amer. Mineral.* **62**, 304-308.

NEILSON, M. J. & HAYNES, S. J. (1973): Biotites in calc-alkaline intrusive rocks. *Mineral. Mag.* **39**, 251-253.

PAPIKE, J. J., ROSS, M. & CLARK, J. R. (1969): Crystal-chemical characterization of clinoamphiboles based on five new structure refinements. *Mineral. Soc. Amer. Spec. Pap.* **2**, 117-136.

RAMBERG, H. (1952): Chemical bonds and distribution of cations in silicates. *J. Geol.* **60**, 331-355.

ROSENBERG, P. E. & FOIT, F. F. JR. (1977): $Fe^{2+}$–F avoidance in silicates. *Geochim. Cosmochim. Acta* **41**, 345-346.

SCOTT, S. D. (1973): Experimental calibration of the sphalerite geobarometer. *Econ. Geol.* **68**, 466-474.

SHIMAZAKI, H. (1968): Geology and ore deposits of the Tsumo Mine, Shimane Prefecture. *Jap. J. Geol. Geog.* **39**, 55-72.

TOULMIN, P. T., III & BARTON, P. B., JR. (1964): A thermodynamic study of pyrite and pyrrhotite. *Geochim. Cosmochim. Acta* **28**, 641-671.

TROLL, G. & GILBERT, M. C. (1972): Fluorine–hydroxyl substitution in tremolite. *Amer. Mineral.* **57**, 1386-1403.

WHEELER, J. O. & GABRIELSE, H., coordinators (1972): The Cordilleran structural province. *In* Variations in Tectonic Styles in Canada (R. A. Price & R. J. W. Douglas, eds.), *Geol. Assoc. Can. Spec. Pap.* **11**.

WILSON, A. D. (1960): The micro-determination of ferrous iron in silicate minerals by a volumetric and a colorimetric method. *The Analyst* **85**, 823-827.

WONES, D. R. & EUGSTER, H. P. (1965): Stability of biotite: experiment, theory, and application. *Amer. Mineral.* **50**, 1228-1272.

ZAW, U KHIN, (1976): *The Cantung E-Zone Orebody, Tungsten, Northwest Territories: A Major Scheelite Skarn Deposit.* M.Sc. thesis, Queen's University, Kingston, Ontario.

——— & CLARK, A. H. (1977): The E–Zone scheelite skarn orebody, Canada Tungsten Mine, Tungsten, Northwest Territories: a petrological and fluid inclusion study. *Geol. Assoc. Can.–Mineral. Assoc. Can. – Soc. Econ. Geol. – Can. Geophys. Union Program Abstr.* **2**, 57.

*Received August 1977; revised manuscript accepted February 1978.*